Electronic Supplementary Material (ESI) for Journal of Materials Chemistry C.

Supplementary Information

Valence state control of Cr^{4+}-activated Li_2SrGeO_4 for NIR-II light source to distinguish deuterium and non-deuterium reagents

Xiaoxuan Guo[a], Bomei Liu[*a,] Rongyi Kuang[a], Weijiang Gan[c], Lin Huang[a], Jing Wang[*ab]

[a]*Ministry of Education Key Laboratory of Bioinorganic and Synthetic Chemistry, State Key Laboratory of Optoelectronic Materials and Technologies, School of Chemistry, Sun Yat-Sen University, Guangzhou 510006, China*
[b] *Nanchang Research Institute, Sun Yat-sen University, Nanchang, Jiangxi, 330099, China*
[c] *Guangxi Academy of Sciences, Nanning, Guangxi, 530007, China.*

Section 1: Figures and tables

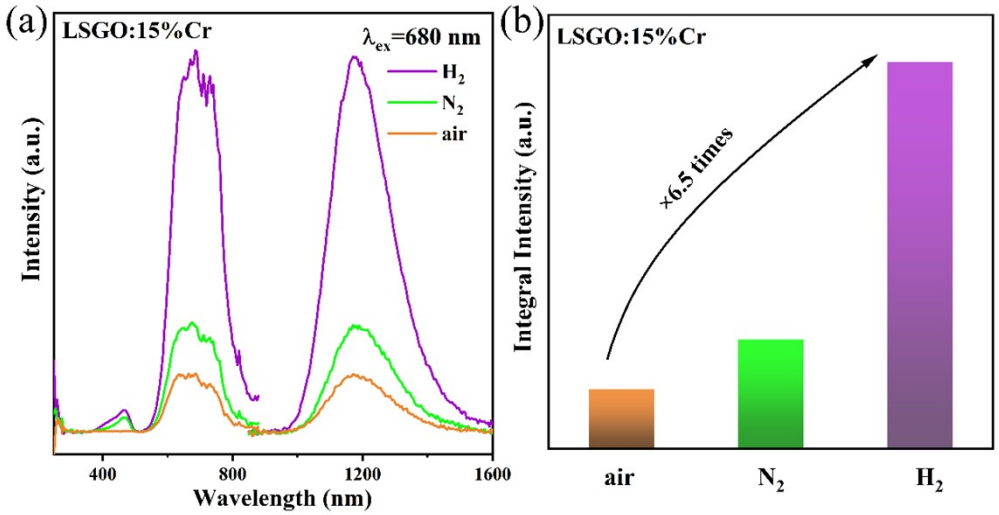

Figure S1. (a) PL/PLE spectra and (b) PL integral intensity of LSGO:15%Cr sintered in air/N_2/H_2 atmosphere.

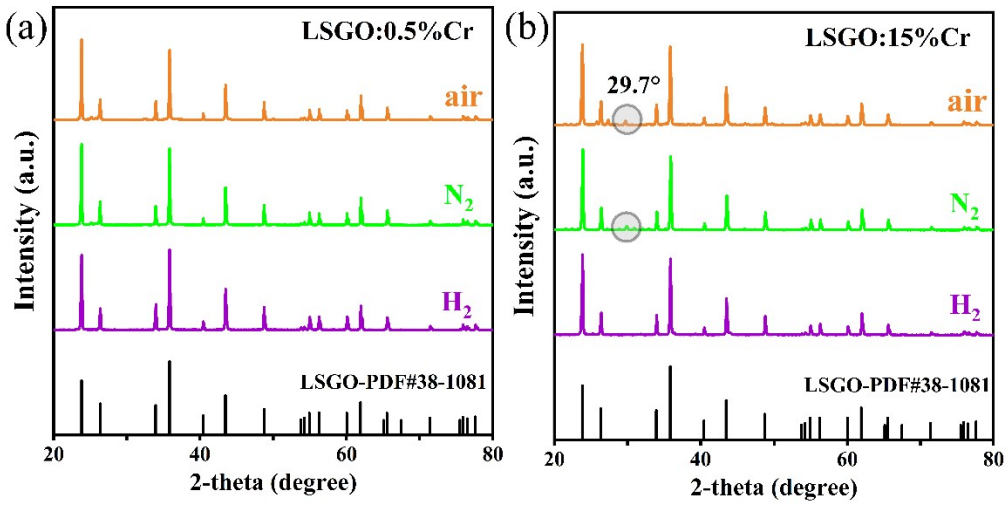

Figure S2. XRD patterns of (a) LSGO:0.5%Cr and (b) LSGO:15%Cr sintered in air/N_2/H_2 atmosphere.

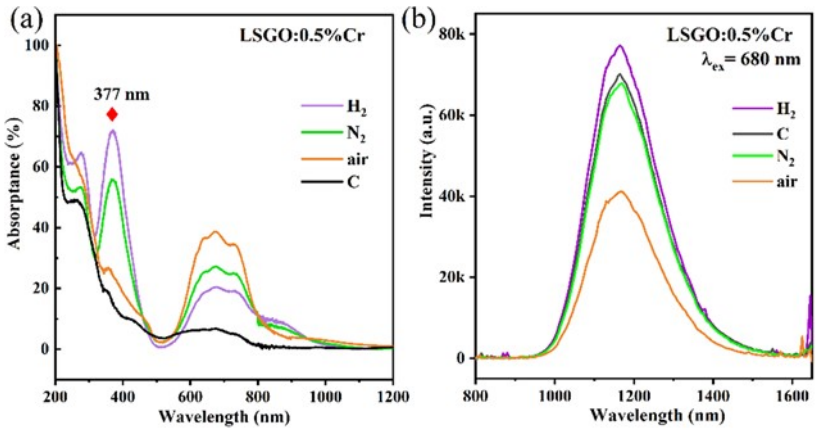

Figure S3. The (a) Abs and (b) PL of LSGO:0.5%Cr sintered in air/N_2/H_2 atmosphere and active carbon.

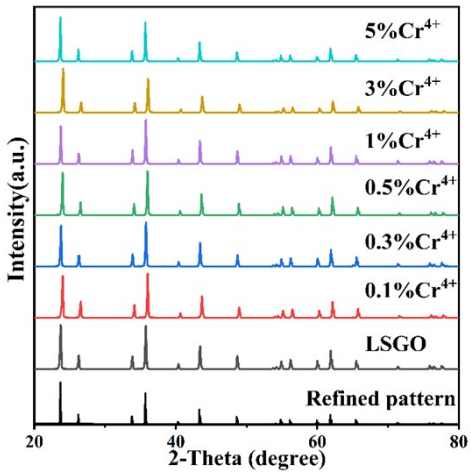

Figure S4. The XRD patterns of LSGO:xCr^{4+} (x = 0-5%) sintered in H_2.

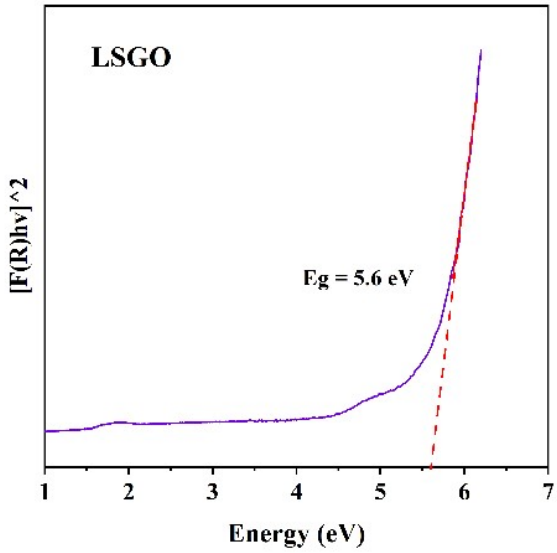

Figure S5 The Abs spectra of LSGO with $[F(R)\times h\nu]^2$ as a function of photon energy for determining the band energy.

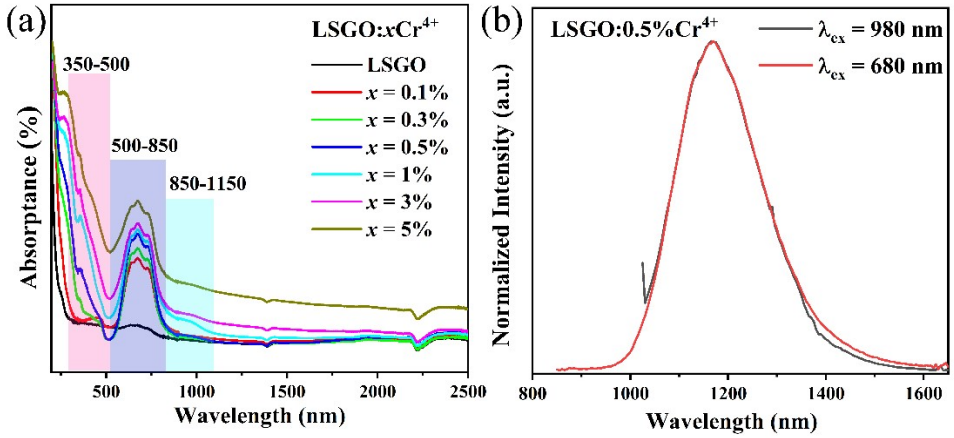

Figure S6. (a) The absorption spectra of LSGO:xCr^{4+} (x = 0-5%). (b) The normalized PL spectra of LSGO:0.5%Cr^{4+} excited at 680nm and 980 nm, respectively.

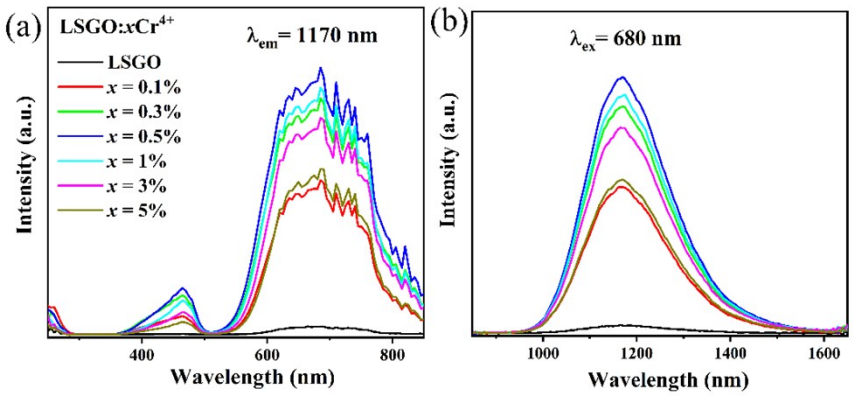

Figure S7. PLE/PL spectra of LSGO:x%Cr^{4+} (x = 0-5%).

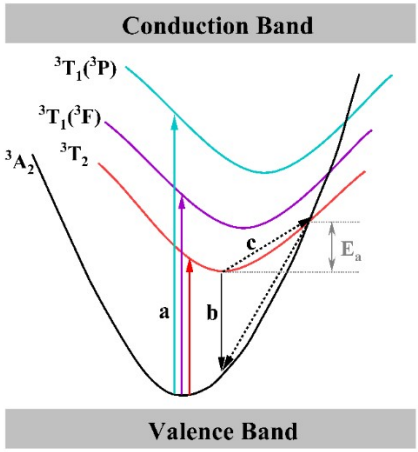

Figure S8. Configuration coordinate diagram of Cr^{4+} to explain the thermal quenching behavior.

Discussion for Figure S8: At low temperature, after excited, a majority of electrons will jump from ground state to excited states and relax to $^3T_2$ level (process a). After that, high-energy electrons will retune to the ground state via radiative transition, along with NIR-II emission (process b). However, in the case of higher temperature, electrons will easily gain more energy to reach the crossover point of $^3T_2$ level and $^3A_2$ level, resulting the nonradiative transition known as the thermal quenching (process c). The higher the crossover point, that is, the larger the value of E_a, the harder it is for electrons to carry out the process c. Therefore, it

can be concluded that the larger activation energy is beneficial to the thermal stability of phosphors.

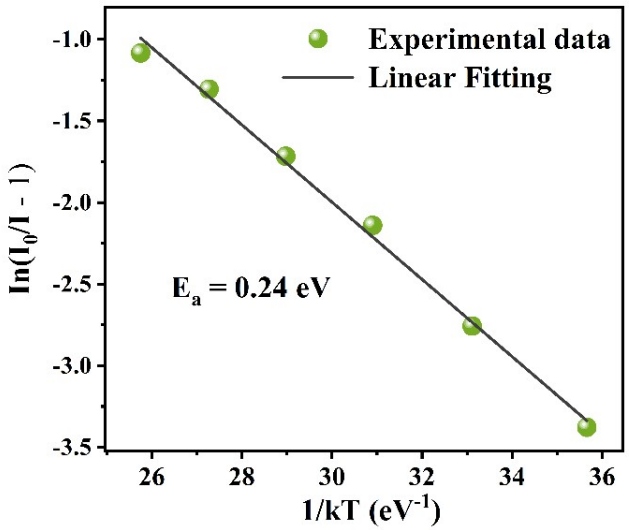

Figure S9. The plot of $\ln(I_0/I - 1)$ versus 1/kT of LSGO:0.5% Cr^{4+}

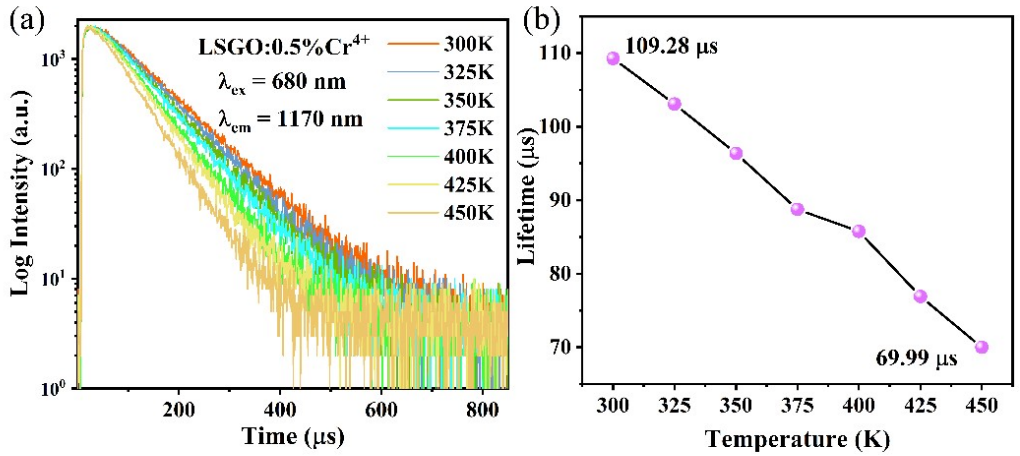

Figure S10. (a) The fluorescent decay curves and (b) the temperature dependent lifetime of LSGO:0.5%Cr^{4+} at difference temperatures.

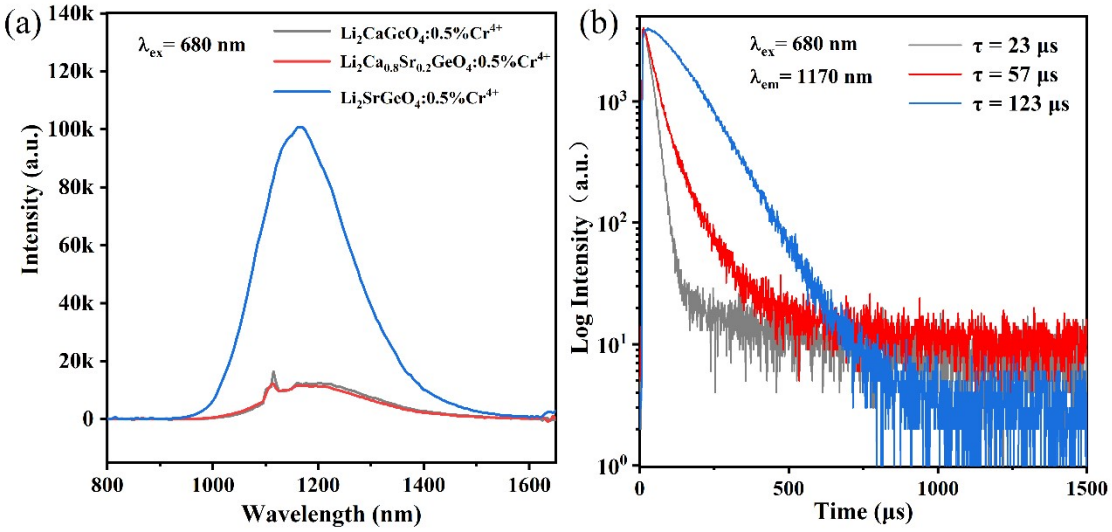

Figure S11. (a) The PL spectra and (b) the fluorescent decay curves of Li_2CaGeO_4:0.5%Cr^{4+}, $Li_2Ca_{0.8}Sr_{0.2}GeO_4$:0.5%$Cr^{4+}$ and Li_2SrGeO_4:0.5%Cr^{4+}.

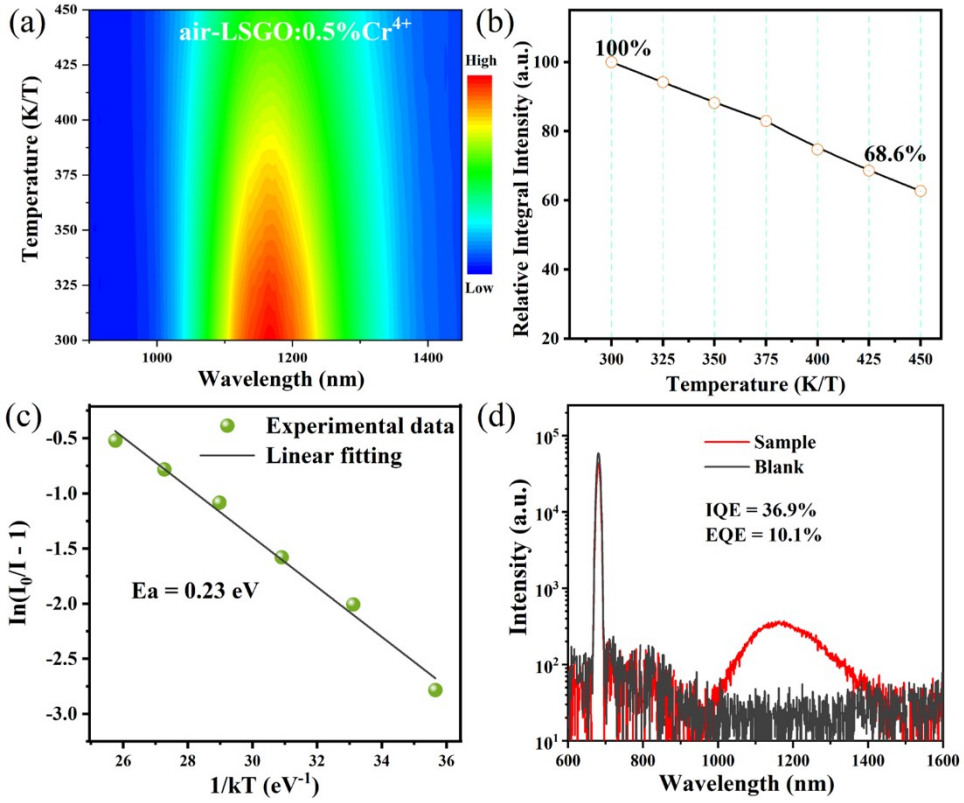

Figure S12. Related data and measurements of the LSGO:0.5%Cr^{4+} phosphor calcined in air atmosphere, including (a) the two-dimensional color map of temperature-dependent emission spectra. (b) relative PL integral intensity at different temperatures. (c) the plot of $\ln(I_0/I - 1)$ versus 1/kT. (d) the measurement of QE excited at 680 nm.

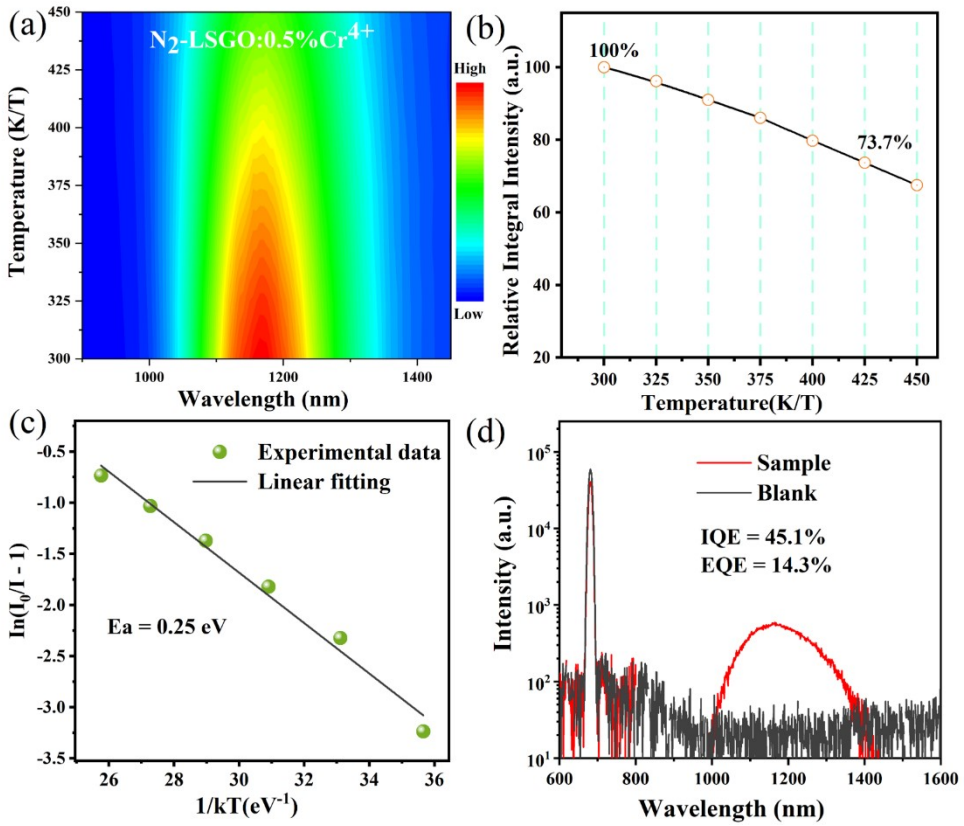

Figure S13. Related data and measurements of the LSGO:0.5%Cr^{4+} phosphor calcined in N_2 atmosphere, including (a) the two-dimensional color map of temperature-dependent emission spectra. (b) relative PL integral intensity at different temperatures. (c) the plot of $\ln(I_0/I - 1)$ versus 1/kT. (d) the measurement of QE excited at 680 nm.

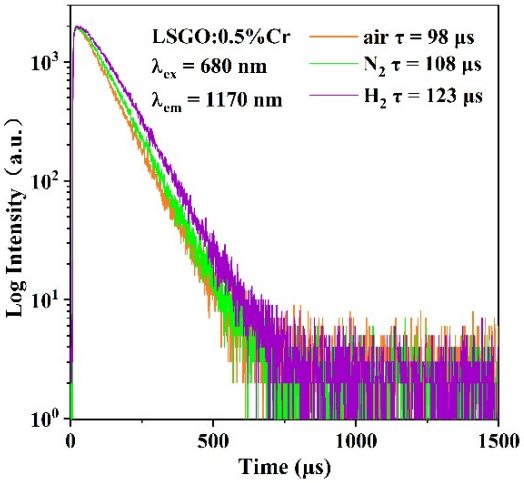

Figure S14. The fluorescent decay curves and lifetime of LSGO:0.5%Cr^{4+} at difference atmospheres.

Table S1. EXAFS fitting parameters at the Cr K-edge for various samples. S_0^2=0.8

Sample	Path	*CN*	*R*(Å)	σ^2(Å^2)	ΔE_0(eV)	*R* factor
Cr_2O_3	Cr-O1	3.0	1.96	0.0088	-3.20	0.0122
	Cr-O2	3.0	1.98	0.0022	-9.05	
CrO_2	Cr-O1	2.0	1.78	0.0124	-8.12	0.0117
	Cr-O2	4.2	1.93	0.0087	-15.09	
Sample	Cr-O	4.1	1.98	0.0024	2.24	0.0171

Table S2. Structural parameters for LSGO refined by Rietveld analysis of powder XRD at room temperature.

Li_2SrGeO_4			**a=b=5.27680Å** **c=6.75400 Å**		**α=β=γ=90°** **V=188.0626 Å^3**	
Atom	*x*	*y*	*z*	Occ.	Wyck	Sym.
Li	0.0000	0.50000	0.25000	1	4d	-4··
Sr	0.0000	0	0.50000	1	2b	-42m
Ge	0.0000	0	0.00000	1	2a	-42m
O	0.19900	0.199000	0.14900	1	8i	··m

Table S3. Bond Length (Å) of LSGO

Vector	**Length(Å)**
Li-O	2.02256
Ge-O	1.79390
Sr-O1	2.79390
Sr-O2	2.46135

Materials	Activator	λ_{ex} (nm)	λ_{em} (nm)	FHWM (nm)	IQE %	EQE %	Reference
$CsPbI_3$	Bi^{3+}	450	1145	450	7.17	—	[1]
$Cs_2AgInCl_6$	Cr^{3+}	760	1010	180	22.03	—	[2]
Li_2ZnGeO_4	Cr^{4+}	675	1230	213	8.86	—	[3]
$CaTiO_3$	Ni^{2+}	375	1377	212	1.4	—	[4]
$SrTiO_3$	Ni^{2+}	375	1311	192	6.5	—	[4]
$Y_3Al_2Ga_3O_{12}$	Ni^{2+}	400	1450	300	54	8.2	[5]
$MgSn_2O_4$	Ni^{2+}	680	1480	297	21.6	4.9	[6]
MgO	Ni^{2+} Cr^{3+}	455	1335	235	92.7	25.9	[7]
$Li_{(0.2)}MgO$	Ni^{2+}	680	1420	350	42.9	9.6	[8]
$Li_{(0.1)}MgO$	Ni^{2+}	680	1340	240	73.2	11.6	[8]
Li_2SrGeO_4	Cr^{4+}	680	1170	208	87.8	30.0	this work

Table S4. Several phosphors reported for NIR-II emission (>1000 nm)

Note: — indicates no reference data. The standard deviation of the IQE is 3.8%

Section 2: Equation

Equation S1: The energetic structure of the d^2 system can be described quantitatively by Dq/B, which can be calculated as follow:

$$E[^3T_1(^3F)] - E[^3A_2(^3F)] = m$$

$$E[^3T_1(^3P)] - E[^3T_1(^3F)] = n$$

$$\frac{Dq}{B} = \frac{27(9m + 9n - \sqrt{-4m^2 - 8mn + 81n^2})}{8(7m + 7n + 3\sqrt{-4m^2 - 8mn + 81n^2}}$$

where Dq is the crystal field strength, B is the Racah parameter. m is the energy of $^3A_2 \rightarrow {}^3T_1(^3F)$. n is the energy difference between $^3T_1(^3P)$ and $^3T_1(^3F)$.

Equation S2. A modified Arrhenius equation

$$I = \frac{I_0}{1 + A \cdot exp(-\frac{E_a}{k \cdot T})}$$

Where I_0 is the initial integrated intensity, I is the integrated intensity at a given testing temperature T, A and k represent the Arrhenius constant and the Boltzmann constant, respectively.

Equation S3. Calculation equation for IQE and EQE.

$$\eta_{IQE} = \frac{\int L_S}{\int E_S - \int E_R}$$

$$\eta_{EQE} = \frac{\int L_S}{\int E_R}$$

Where, L_S is the emission spectrum of the sample; E_S and E_R represent the spectra of the given excitation with and without the sample, respectively.

Reference

1 F.-P. Zhu, Z.-J. Yong, B.-M. Liu, Y.-M. Chen, Y. Zhou, J.-P. Ma, H.-T. Sun and Y.-Z. Fang, *Optics Express*, 2017, **25**, 33283-33289.

2 F. Zhao, Z. Song, J. Zhao and Q. Liu, *Inorganic Chemistry Frontiers*, 2019, **6**, 3621-3628.

3 S. Yuan, Z. Mu, L. Lou, S. Zhao, D. Zhu and F. Wu, *Ceramics International*, 2022, **48**, 26884-26893.

4 Y. Gao, B. Wang, L. Liu and K. Shinozaki, *Journal of Luminescence*, 2021, **238**.

5 L. Yuan, Y. Jin, H. Wu, K. Deng, B. Qu, L. Chen, Y. Hu and R.-S. Liu, *Acs Applied Materials & Interfaces*, 2022, **14**, 4265-4275.

6 B.-M. Liu, X.-X. Guo, L. Huang, R.-F. Zhou, R. Zou, C.-G. Ma and J. Wang, *Advanced Materials Technologies*, 2022, 2201181.

7 B.-M. Liu, X.-X. Guo, L.-Y. Cao, L. Huang, R. Zou, Z. Zhou, J. Wang, *Chemical Engineering Journal*, 2023, **452**, 139313.

8 B.-M. Liu, S.-M. Gu, L. Huang, R.-F. Zhou, Z. Zhou, C.-G. Ma, R. Zou and J. Wang, *Cell Reports Physical Science*, 2022, **3**, 101078